

In situ observations of diurnal warming in the skin layer

Chelle L. Gentemann^{1,2} and Peter J. Minnett¹

¹University of Miami, RSMAS, 4600 Rickenbacker Causeway; Miami, FL 33149
(707) 545-2904x14;gentemann@remss.com

²Also at Remote Sensing Systems 438 First St. Suite 200; Santa Rosa, CA 95401

ABSTRACT - Observations of diurnal temperature variability in the oceanic skin layer have been primarily available only from satellite SST retrievals themselves. Since most satellite observations revisit the same location only infrequently, determining how the ocean surface diurnal heating responds to variability in forcing (mainly insolation and wind speed) has been primarily addressed through theoretical modeling or extrapolation of results from *in situ* (buoy) observations measured 0.5 m to 1.5 m below the skin layer. Diurnal heating in the skin layer may be quite different than heating at 0.5 m as this layer responds very rapidly to changes in heat and momentum. The *Explorer of the Seas*, a cruise ship, makes weekly cruises on two alternating tracks through the Caribbean Sea. Measurements from the Marine Atmospheric Emitted Radiance Interferometer (M-AERI) carried on the *Explorer of the Seas* provide one of the few skin SST data sets, along with ancillary measurements necessary for diurnal investigations. Initial analyses show that the surface signature of diurnal warming in the skin layer is chiefly controlled by the wind speed. The daily peak in diurnal warming is directly related to the minimum wind speed during the day, causing the time of the peak to shift depending on when the minimum winds occur. Fluctuations in wind speed can result in multiple peaks in diurnal heating during a single afternoon. Wind speed is negatively lag-correlated with diurnal warming while insolation is positively lag-correlated. The maximum lag-correlation of wind speed (insolation) with diurnal warming is at a time lag of 30 (50) minutes.

I. BACKGROUND

During the day, in clear sky, calm conditions, thermal re-stratification of the top few meters of the ocean will occur. The existence of this diurnal warm layer was first recognized in 1942 [Sverdrup *et al.*, 1942] and has been studied extensively since [Defant, 1961; Woods and Barkmann, 1986; Schluessel *et al.*, 1990; Fairall *et al.*, 1996]. Surface temperature deviations greater than 3K, referenced to subsurface temperatures are not uncommon (e.g., Yokoyama, *et al.*, 1995; Minnett, 2003) and may persist for hours. The omission of a diurnal cycle in SSTs can lead to errors in determining surface fluxes for numerical weather prediction (NWP) and climate models [Webster *et al.*, 1996]. Global SSTs are commonly derived from satellite retrievals which measure at a depth of a few microns, in the infrared to millimeters, in the microwave. Simply averaging day and nighttime observations in regions with diurnal warming will lead to warm biases in the SSTs; therefore correct utilization of the daytime measurements necessitates a model of diurnal warming that is present at these depths.

Several one-dimensional theoretical models have been developed to describe the diurnal warm layer, [Price *et al.*, 1986; Large *et al.* [1994]. While often able to accurately reproduce diurnal warming [Anderson *et al.* 1996; Weller and Anderson, 1996], theoretical diurnal models are difficult to run over large regions where accurate estimates of incident radiation, surface fluxes of sensible heat, latent heat, fresh water, and momentum, and vertical subsurface profiles of temperature, salinity, turbidity, and velocity are not usually available. This has led to interest in developing simplified models of diurnal warming that could be used to estimate global diurnal warming, in the absence of a full set of forcing fields.

Several simplified empirical models of diurnal warming, based on *in situ* and satellite data, have been developed [Webster *et al.*, 1996; Kawai and Kawamura, 2002]. While these simplified models are applicable in some situations, each has drawbacks. Several of the models use daily average forcing fields and do not adequately describe the variability in diurnal warming present within a single day. Another model, developed from *in situ* observations below the skin layer, ascribes a shape to the diurnal warming based on four daily Numerical Weather Prediction (NWP) insolation values, which are notoriously poor, and NWP winds. The correlation between 6 hourly winds and diurnal warming within the skin layer has not been well-established. While including wind history and insolation history should lead to a better model of diurnal amplitudes, it is likely that the thermal response of the skin layer is affected by a more recent history (a few tens of minutes), that is not captured by the 6-hour NWP fields.

Observation have shown that the vertical profile of diurnal warming in the upper ocean is highly variable (Minnett and Ward, 2000) and therefore models developed from *in situ* observations at depth may

not describe the variability within the skin layer. The validity of both the theoretical and empirical models in the skin layer has been explored by a limited number of studies. Using data from two cruises, Minnett (2003) examined diurnal warming using the difference between M-AERI skin and thermosalinograph bulk temperatures. Diurnal warming as large as 4 K was found, relative to a 3-m bulk temperature, and measurable warming was present at wind speeds up to 5-6 ms^{-1} . Donlon *et. al.* (2002) examined a larger dataset of 6 cruises, using a number of different shipboard radiometers capable of accurately measuring skin temperature, and found measurable diurnal warming at wind speeds below 6 ms^{-1} . In this study we use over four years of radiometric skin SST measurements to examine the temporal variability in diurnal warming of the skin layer.

II. DATA

Skin SST observations are from the Marine-Atmosphere Emitted Radiance Interferometer (M-AERI). M-AERI is a Fourier-Transform Interferometric Spectroradiometer that measures radiation at 3-18 μm wavelength. SST is retrieved using a sea and sky view data at 7.7 μm [Minnett *et al.*, 2001]. The M-AERI is mounted on the starboard side of the *Explorer of the Seas*, and has been providing data since late 2000. The ship also has instruments to measure bulk SST, wind speeds, and radiation. Bulk SST is measured by a thermosalinograph located in the bow thruster seawater intake; this is on the starboard side of the ship, forward from the M-AERI instrument. When the intake flow is low, the bulk SST is warmed by the ship. Since mid-2002, intake flow rate is available and the bulk SST is flagged when flow rates fall below 15 Lmin^{-1} . For earlier data, bulk SST data was visually flagged. Both bulk and skin SSTs are flagged when the ship is within 20 km of a port as the data may become influenced by shallow water and land effects. Wind speed and direction are available from three anemometers on the ship, one located at the bow and two located on the main mast. All winds are corrected for ship motion. The bow wind speed is measured at 24 m above the waterline while the port and starboard winds are at 45 m. Wind speeds are converted to a 10 m height using a logarithmic profile. The main mast is also instrumented to measure incident radiation using Eppley radiometers. The ship's cruise tracks are shown in Figure 1. During each weekly cruise, the ship makes two long daytime cruises to and from its main destination and these segments represent the majority of valid daytime data.

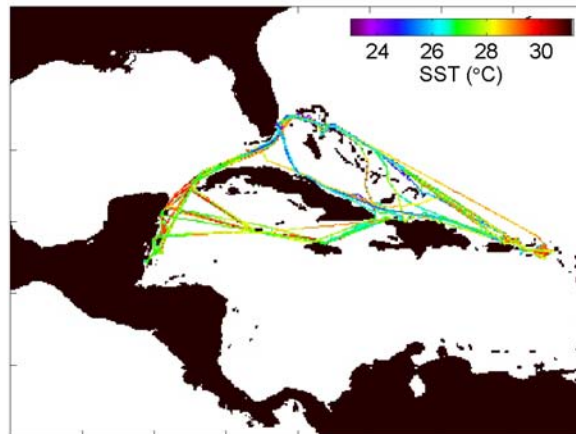


Figure 1. SST along cruise tracks for the *Explorer of the Seas*. Data taken when the ship is in port are not usable, and the diurnal warming analyzed here are from the two days each week that the ship travels to and from Miami on the longer legs. The measured temperature is indicated by color.

III. RESULTS

There are 44 days with significant diurnal warming in the dataset. Figure 2A shows the skin minus bulk SST as a function of local time with wind speed indicated by color. At high wind speeds ($>10 \text{ms}^{-1}$), as indicated by the blue-green dots, there is no diurnal cycle and the difference is constant at all local times. The skin is almost always cooler than the bulk SSTs, and here the mean difference is -0.23 K. Some of the variability between the skin and bulk SSTs at higher wind speeds is partially due to the instrument location. Diurnal warming is clearly present at low wind speeds (red-orange dots) between 10 AM and 6 PM. The peak warming is 3.25 K and occurs at a local time of 12:22 PM at a wind speed of 4.5 ms^{-1} . The wind speed was very low in the morning and increased slightly by midday.

Figure 2B shows the differences, skin minus bulk, as a function of wind speed with local time indicated by color. In the morning and evening (blue-green) the mean difference is essentially constant. The increase in the difference between skin and bulk temperatures usually seen at low wind speeds is not so obvious in these data. At midday (red-orange) there is diurnal warming at low wind speeds. At lower instantaneous wind speeds, it appears that the diurnal warming is less, which is counter to the findings of researchers who have found larger diurnal warming at low wind speeds. There are no days with constant winds $<2 \text{ ms}^{-1}$; the few cases for winds $<2 \text{ ms}^{-1}$ are for days when the wind dropped briefly and diurnal warming was quickly established, but not observed to be as large as in situations with persistent low winds.

Figure 3 shows how the diurnal warming magnitude responds to changes in wind and insolation. Since the *Explorer of the Seas* is a large vessel, it is not immediately clear which of the three wind speed measurements should be best to use. The bow wind speed is closest to sea level, but the port and starboard may be subjected to less flow distortion. All three have been plotted in Figure 3 (blue/cyan/green lines). Figure 3A shows decreasing winds through the morning and an increasing diurnal warming (black line). As the wind decreases and insolation increases, diurnal warming steadily increases from 9 AM to 10:42 AM, after which the wind speed increases and diurnal warming rapidly decreases. The wind speed continues increasing to a value of 6.5 ms^{-1} , and within 10 minutes of it reaching this value, the diurnal warm layer has been completely erased from the skin SST measurement. The maximum warming on this day was not large, 0.65 K , since the minimum in wind speed occurred early in the day when insolation was weak. Cloud causes the insolation to drop by 100 Wm^{-2} just before the peak in diurnal warming but there is no real change in the slope of the increase in diurnal warming indicating that changes in insolation of less than 100 Wm^{-2} may not have a marked effect on the warming. The insolation drops to 650 Wm^{-2} just as the diurnal peak starts to diminish, but then it climbs to 1000 Wm^{-2} . In this case, the increase in wind speed had a much stronger effect on the diurnal warming, since even as the insolation was increasing from 650 Wm^{-2} to 1000 Wm^{-2} the diurnal warming was quickly diminishing.

Figure 3B shows a double peak in diurnal warming. The wind speeds are less than 1 ms^{-1} and the surface rapidly warms, increasing by 2.15 K at 10:36 AM. The start in the decrease in diurnal warming appears to be linked to an

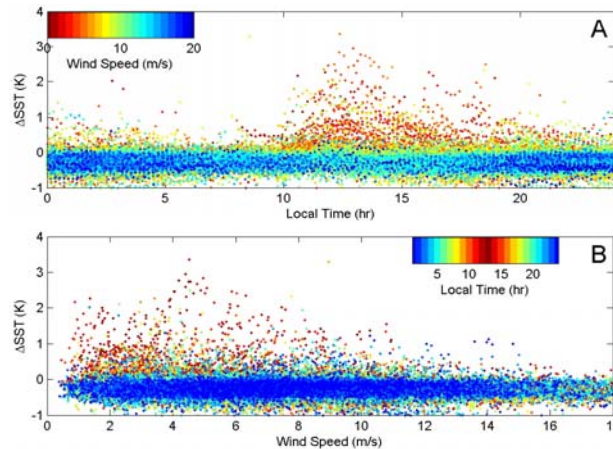


Figure 2. Diurnal warming as a function of local time and wind speed. The difference, skin minus bulk SST is shown 2A, with wind speed indicated by dot color and in 2B as a function of wind speed with local time indicated by dot color.

increase in the measurements of wind speed. The insolation is continually increasing throughout this episode. The *Explorer of the Seas* is a large vessel and the differences in the wind speeds measurements are attributable to the different locations of the anemometers. The winds continue increasing until 1:10 PM and the diurnal warming decreases until 1:20 PM. As winds begin decreasing, there is a lag of about ten minute before increases in warming. There is a second diurnal peak at 2:40 PM. For this peak, the winds begin increasing about 20 minutes before the diurnal warming begins decreasing.

Figure 3C illustrates a case similar to that in 3B, showing two diurnal peaks. But in this example the larger peak is after the smaller peak. Again in this case the changes in wind speed and diurnal warming lag each other by 10-20 minutes. The first peak occurs at 9:55 AM, with winds just below 3 ms^{-1} . The second peak occurs at 3:35 PM, but is preceded by several large fluctuations in diurnal warming that are not related

to any obvious fluctuations in wind speed. The variations in diurnal warming during the second peak are correlated with variations in insolation, on the order of 350 Wm^{-2} , 30-40 minutes prior. In this example, variation in diurnal warming lags variation in winds at about half the lag for insolation. Wind-induced mixing may erase surface warming rapidly, while, in the absence of wind mixing, changes in radiative forcing take almost twice as long to result in measurable changes simply due to thermal inertia..

Figure 3D reveals single diurnal peak of 1.3 K at 12:20 PM with wind speeds fairly constant at roughly 2 ms^{-1} . The day had clear skies and the insolation follows the expected smooth curve. The maximum insolation occurs at 11:40 AM, 40 minutes before the diurnal maximum in skin temperature.

Figure 3E also shows well-defined diurnal warming, but with two equal peaks of 1.7 K at 1 PM and 1:40 PM. The port and starboard wind speeds increase simultaneously with the decrease in diurnal warming. The bow wind speed does

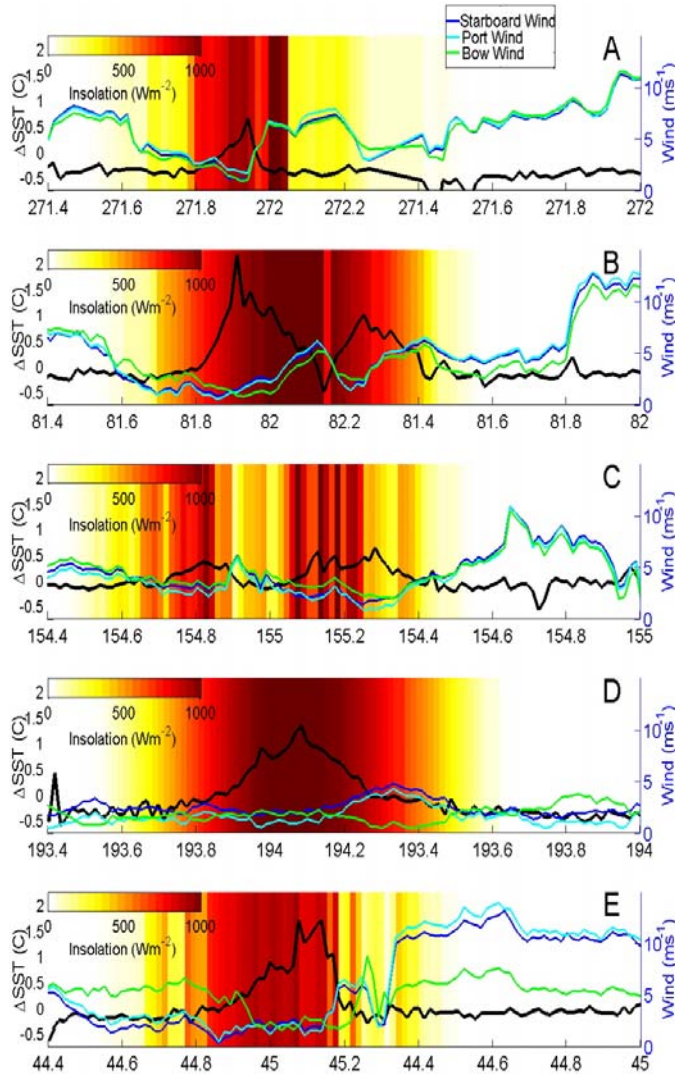


Figure 3. Several examples of diurnal warming from the *Explorer of the Seas*. The difference, skin minus bulk, is shown on the left axis in black, the wind speed is shown on the right axis in blue, cyan, and green, the insolation is indicated by color in the background, and day of the year is indicated. Panel A is from 2001, panels B-D are from 2002, and panel E is from 2003.

not begin increasing until 2:20 PM. The fluctuations in diurnal warming in the morning and late afternoon are correlated with variations in the insolation, again lagged by 40 minutes. The insolation changes by $100\text{-}200 \text{ Wm}^{-2}$ are associated with changes in diurnal warming on the order of 0.1 to 0.2 K.

The temporal lagged correlation between a) insolation and diurnal warming and b) wind speed and diurnal warming was calculated using all 44 days with significant diurnal warming, using daytime measurements only. Correlations with diurnal warming were positive for insolation and negative for wind speed, meaning that as insolation increases the surface warms, whereas increasing wind speed leads to diminished diurnal warming. The strongest correlations occurred for lags of 50 minutes for the insolation and 30 minutes for the wind speed. The lag-correlation for insolation is half its peak value in 2.5 hours and not statistically significant after 3.3 hours. The lag-correlation for wind speed is half its peak value in 3.6 hours and not statistically significant after 6.6 hours. These long-tails may be partially due to the auto-correlation in the forcing fields..

IV. CONCLUSIONS

Initial results show that the surface signature of diurnal warming is primarily related to wind speed and secondarily to insolation. Relatively small changes in wind speed rapidly and strongly affect the amount of diurnal warming present in the skin layer. The daily peak in diurnal warming is directly related to the minimum wind speed during the day, causing the time of the peak to shift depending on when the minimum winds occur. Fluctuations in wind speed can result in multiple peaks in diurnal heating. When the wind speed rapidly increases to above 6 ms^{-1} , warming can be completely erased from the skin SST measurement in as quickly as 30 minutes. For all the days with diurnal warming the strongest lag-correlation between wind speed and diurnal warming occurred at 30 minutes. Fluctuations in insolation need to be large (over 100 Wm^{-2}) to cause a measurable effect (0.1 to 0.2 K) on the diurnal signal and the strongest correlation at a 50 minute lag. These results imply that near-simultaneous wind and insolation observations are important for accurately modeling diurnal warming. Future work will include comparing this data to several of the empirical diurnal warming models that have been developed and specifically simplified for global, near-real-time application to satellite SST observations.

V. ACKNOWLEDGEMENTS

Thank you to Eddie Kearns, Chip Maxwell, and Don Cucchiara for the *Explorer of the Seas* data. This work was supported by funding from NOAA (NA030AR4310126) and NASA (NM0710772, NAG5-11104 and NNG04HZ33C).

VI. REFERENCES

- Anderson, S. P., R. A. Weller, et al. (1996). "Surface Buoyancy Forcing and the Mixed Layer of the Western Pacific Warm Pool: Observations and 1D Model Results." *J. Climate* 9(12): 3056-3085.
- Defant, A., *Physical Oceanography*, Vol.2, 728 pp., Pergamon, Oxford, 1961.
- Donlon, C. J., P. J. Minnett, et al. (2002). "Toward Improved Validation of Satellite Sea Surface Skin Temperature Measurements for Climate Research." *J. Climate* 15(4): 353-369.
- Fairall, C. W., E. F. Bradley, et al. (1996). "Cool skin and warm layer effects on sea surface temperature." *J. Geophys. Res.* 101(C1): 1295-1308.
- Kawai, Y., H. Kawamura, (2002), "Evaluation of the diurnal warming of sea surface temperature using satellite-derived marine meteorological data", *J. Oceanogr.*, 58, 805-814.
- Large, W., J. C. McWilliams and S. C. Doney, (1994): Oceanic vertical mixing: A review and model with nonlocal boundary layer parameterization, *Rev. of Geophys.*, 32, 363-403.
- Price, J. F., R. A. Weller, et al. (1986). "Diurnal Cycling: Observations and models of the upper ocean response to diurnal heating, cooling, and wind mixing." *J. Geophys. Res.* 91: 8411-8427.
- Minnett, P.J., "Radiometric measurements of the sea-surface skin temperature: the competing roles of the diurnal thermocline and the cool skin", (2003) *Inter. J. Rem. Sens.*, 24(24), pp 15033-47.
- Minnett, P. J., R. O. Knuteson, F.A. Best, B.J. Osborne, J. A. Hanafin and O. B. Brown, (2001). The Marine-Atmosphere Emitted Radiance Interferometer (M-AERI), a high-accuracy, sea-going infrared spectroradiometer. *Journal of Atmospheric and Oceanic Technology*, 18, 994-1013.
- Minnett, P.J., and B. Ward, "Measurements of near-surface ocean temperature variability -Consequences on the validation of AATSR on Envisat". In *Proceedings of ERS - ENVISAT Symposium "Looking down to Earth in the New Millennium"*, European Space Agency. Gothenburg, Sweden, 2000, SP-461. 10pp. Available as CD-ROM from ESA Publications Division, ESTEC, PO Box 299, 2200 AG Noordwijk, The Netherlands.
- Schluessel, P., W. J. Emery, H. Grassl, and T. Mammen, 1990. On the skin-bulk temperature difference and its impact on satellite remote sensing of sea surface temperature. *J. Geophys. Res.*, Vol. 95, pp. 13,341-13,356.

- Sverdrup, H.U., M.W. Johnson and R.H. Fleming, 1942: *The Oceans, Their Physics, Chemistry, and General Biology*. Prentice Hall, New York, 1087 pp.
- Webster, P. J., C. A. Clayson, et al. (1996). "Clouds, radiation, and the diurnal cycle of sea surface temperature in the tropical western Pacific." *J. Climate* 9: 1712-1730.
- Weller, R. A. and S. P. Anderson (1996). "Surface Meteorology and Air-Sea Fluxes in the Western Equatorial Pacific Warm Pool during the TOGA Coupled Ocean-Atmosphere Response Experiment." *J. Climate* 9(8): 1959-1990.
- Wick, G.A., (2003) "Inter-comparison of the performance of numerical models for diurnal warming using detailed near-surface temperature measurements", *Eos Trans. AGU*, 84(52), Ocean Sci. Meet. Suppl., Abstract OS311-07.
- Woods, J. D. and W. Barkmann (1986). "The response of the upper ocean to solar heating. I: The mixed layer." *Q. J. R. Meteorol. Soc.* 112: 1-27.
- Yokoyama, R., S. Tanba, et al. (1995). "Sea surface effects on the sea surface temperature estimation by remote sensing." *International Journal of Remote Sensing* 16: 227-23.